miR-124 targets retinoid X receptor α to reduce growth of TSC2-deficient lymphangioleiomyomatosis

JIA LIU[1*], JUN YUAN[2*], TIANXIANG FENG[3], YINJUAN ZHAO[4-6], QIAN SUN[3], JUN CHEN[7,8], JINGYU CHEN[9], MEILING JIN[10] and BIN XUE[3,8,11,12]

[1]MOE Key Laboratory of Model Animal for Disease Study, Model Animal Research Center, Nanjing University, Nanjing, Jiangsu 210093; [2]Biochemical and Environmental Engineering School of Xiaozhuang Collage, Nanjing, Jiangsu 211171; [3]Jiangsu Key Laboratory of Molecular Medicine, School of Medicine, Nanjing University, Nanjing, Jiangsu 210093; [4]Collaborative Innovation Center of Sustainable Forestry in Southern China; [5]Institute of Forest Protection, College of Forestry, Nanjing Forestry University; [6]Jiangsu Key Laboratory for Prevention and Management of Invasive Species, Nanjing, Jiangsu 210037; [7]Department of Pathology, The Affiliated Drum Tower Hospital, Medical School of Nanjing University, Nanjing, Jiangsu 210008; [8]Liver Disease Collaborative Research Platform of Medical School, Nanjing University, Nanjing, Jiangsu 210093; [9]Department of Cardiothoracic Surgery, Lung Transplant Group, Wuxi People's Hospital, Nanjing Medical University, Wuxi, Jiangsu 214023; [10]Pulmonary Department, Zhongshan Hospital, Fudan University, Shanghai 200032; [11]State Key Laboratory of Pharmaceutical Biotechnology, Nanjing University, Nanjing, Jiangsu 210093; [12]State Key Laboratory of Natural Medicines, China Pharmaceutical University, Nanjing, Jiangsu 210009, P.R. China

Received August 7, 2018; Accepted November 22, 2018

DOI: 10.3892/or.2018.6916

Abstract. Lymphangioleiomyomatosis (LAM) is a rare neoplastic disease that leads to progressive destruction of lung function. However, the mechanisms underlying the progression of LAM remain unknown. Recent studies demonstrated that miR-124-3p (hereinafter referred to as miR-124) is a downregulated miRNA in tumors and it is still unclear whether miR-124 participates in LAM. In the present study, it was revealed that miR-124 was downregulated in LAM specimens and overexpression of miR-124 resulted in the apoptosis of TSC2-deficient cells via *RXRα* (retinoid X receptor α), while slightly influencing TSC2 wild-type cells. Furthermore, a xenograft model demonstrated that the miR-124/RXRα axis regulated the growth and fatty acid oxidation genes in TSC2-null cells. Altogether, our results revealed the suppressive functions and mechanisms of miR-124 in LAM progression, providing novel therapeutic targets for LAM treatment.

Correspondence to: Professor Bin Xue, Jiangsu Key Laboratory of Molecular Medicine, School of Medicine, Nanjing University, 22 Hankou Road, Nanjing, Jiangsu 210093, P.R. China
E-mail: xuebin@nju.edu.cn

Professor Meiling Jin, Pulmonary Department, Zhongshan Hospital, Fudan University, 180 Fenglin Road, Shanghai 200032, P.R. China
E-mail: mljin118@163.com

*Contributed equally

Key words: lymphangioleiomyomatosis, miR-124, retinoid X receptor α

Introduction

Lymphangioleiomyomatosis (LAM) is a multisystem disorder with a prevalence of 1-2.6 cases/1,000,000 women (1,2). LAM is characterized by proliferation of abnormal smooth muscle-like cells, which leads to lung cysts and lung parenchyma destruction (3). Women with LAM can also develop renal angiomyolipomas (AML) (4). LAM can occur in a sporadic form or in association with germline mutations in the tuberous sclerosis complex (TSC) genes (5). Combination of typical high resolution CT scan with invasive biomarker vascular endothelial growth factor D may help the future diagnosis of LAM (3). Rapamycin is a promising medication as the mammalian target of rapamycin complex 1 (mTORC1)-inhibitor, which promotes lung function and inhibits regrowth of angiomyolipoma (AML) (6). A recent study demonstrated that rapamycin upregulated multiple microRNAs (miRNAs), including pro-survival miRNAs in TSC2-deficient patient-derived cells (7), providing a possible explanation for the relapse in patients receiving rapamycin therapy. To date, lung transplantation is still the best choice for the treatment of LAM at an advanced phase. Therefore, to develop new therapies, elucidating the central regulatory mechanism of LAM growth is urgently needed. A previous study revealed that miR-25 targeted TSC1 in LAM cells (4), implying the potential to develop new molecular miRNA-targeted LAM therapies. miRNAs are small non-coding RNAs that typically inhibit the

translation of messenger RNAs (mRNAs) by binding to the 3'-untranslated regions (UTRs) (5,8). Dysregulated miRNAs may lead to the initiation and maintenance of diseases (9). It is well known that miRNAs participate in human carcinogenesis as either tumor suppressors or oncogenes. Recent studies revealed that decreased expression of miR-124 was related to carcinogenesis and that it functioned as a tumor suppressor in hepatocellular carcinoma, colorectal, bladder and breast cancer (6,7,9-11). However, the exact role of miR-124 in LAM progression is not fully understood.

In the present study, we demonstrated the decreased expression of miR-124 in LAM specimens. Ectopic overexpression of miR-124 induced the apoptosis of TSC2-deficient cells via retinoid X receptor α (RXRα) while only slightly influencing the TSC2 wild-type cells both *in vitro* and *in vivo*. Additionally, we found that the miR-124/RXRα axis regulated fatty acid oxidation in TSC2-null cells. Our results provide valuable clues for understanding the suppressive functions and underlying mechanisms of miR-124 in LAM. Notably, increased expression of miR-124 and RXRα may serve as promising predictors for LAM prognosis.

Materials and methods

Human specimens. Human female AML (n=41) samples were recruited at the Department of Pathology of Nanjing Drum Tower Hospital from January 2008 to December 2017 (age, 30-50 years). Human female LAM (n=4) and normal lung tissues (n=5) used in this study were collected from LAM patients and healthy donors at Wuxi People's Hospital from January 2008 to December 2017 (age, 30-50 years). This study was approved by the Scientific Research Ethics Committee of the Affiliated Drum Tower Hospital, Medical School of Nanjing University. Informed consents were obtained from all participants.

Animals. Fifteen 6-week-old male BALB/c-nu/nu were purchased from Nanjing Biomedical Research Institute (NBRI) of Nanjing University (Nanjing, China) (weight, 18-19 g), and were maintained on a normal 12-h light/dark schedule at a constant temperature and humidity. The housing conditions met the specific pathogen-free (SPF) standards. All mice were maintained on a regular chow diet and water *ad libitum*. Animals were sacrificed when the tumors reached 1.5 cm^3. All animal procedures were carried out in accordance with the approval of the Animal Care and Use Committee at the Model Animal Research Center of Nanjing University.

Cell culture and transfection. TSC2 wild-type/p53-null and TSC2-null/p53-null mouse embryonic fibroblasts (generously provided by Dr John Blenis, Harvard University, Boston, MA, USA) were cultured in Dulbecco's modified Eagle's medium (DMEM) medium supplemented with 10% fetal bovine serum (FBS). LAM patient-derived 621-101 cells (provided by Dr John Blenis) were cultured in IIA complete medium in a 37˚C incubator with 5% CO_2 and a humidified atmosphere.

For the transfection of pcDNA3.3-*RXRα* and miR-124 mimics, cells were transfected with pcDNA3.3-*RXRα* (1/2 μg) and miR-124 mimics (final concentration of 20 nM) using Lipofectamine 2000 reagent (Life Technologies; Thermo Fisher Scientific, Inc., Waltham, MA, USA). The empty pcDNA3.3 and scramble sequence of miRNA mimics were used as the negative controls (NCs). Cells were treated with rapamycin (Sigma-Aldrich; Merck KGaA, Darmstadt, Germany) at 20 nM for 48 h. An equivalent volume of dimethyl sulphoxide (DMSO) was delivered in a vehicle control group. Cell morphology was observed under a fluorescence microscope (CKX41; Olympus Corp., Tokyo, Japan).

Establishment of tumor-bearing mice. Inducible TSC2-null cells expressing miR-124 (designated as TSC2 Null-tet-124) were established. Each mouse (male BALB/c-nu/nu, 6-weeks-old) was subcutaneously injected in the lower back with $1x10^7$ TSC2 null-tet-124 cells diluted in 200 μl DMEM. After 7 days, the nude mice bearing tumors were randomly divided into 2 groups (5-7/group). One group received doxycycline (Dox) treatment (1 mg/ml Dox in drinking water) to induce the miR-124 expression. The other group was not treated with Dox and was set as the negative control group. The tumor volume was assessed every 4 days. Tumor-bearing mice were sacrificed under deep anesthesia with pentobarbital sodium at 31 days after inoculation, and then the tumors were dissected, weighed and kept at -80˚C for further study.

Cell apoptosis assay. Cells were harvested at 48 h after transfection and collected by 160 x g centrifugation. Cells were washed with phosphate-buffered saline (PBS) and resuspended in 500 μl binding buffer. Then, 5 μl of Annexin V-FITC and 5 μl of propidium iodide (PI) (Nanjing KeyGen Biotech Co., Ltd., Nanjing, China) were added. The cells were incubated in the dark for 10 min, and then subjected to flow cytometric analysis. Cell morphology was observed under a fluorescence microscope (Olympus CKX41; Olympus Corp.).

Assessment of cellular ATP level. The cellular ATP level was determined using the ATP Determination kit (Invitrogen; Thermo Fisher Scientific, Inc.). All values were normalized to total protein levels.

cDNA microarray. Total RNA was extracted using TRIzol reagent and then reverse transcribed to cDNA using PrimeScript RT Master Mix (both from Takara Bio, Inc., Otsu, Japan). cDNA microarray analysis of TSC2 wild-type and TSC2-null cells transfected with miR-124 mimics was performed by Shanghai Biotechnology Corp. (Shanghai, China).

Quantitative RT-PCR. The cDNA was subjected to real-time PCR using the SYBR-Green PCR kit (Takara Bio, Inc.) with the ABI PRISM 7300 Sequence Detector under the following thermocycling conditions: 95˚C for 5 min, then 35 cycles of 95˚C for 15 sec, 58˚C 15 sec, 72˚C for 30 sec and a final extension at 72˚C for 5 min. The following primers were used: *RXRα* (mouse) 5'-ATGGACACCAAACATTTCCTGC-3' (forward), and 5'-CCAGTGGAGAGCCGATTCC-3' (reverse); *Acox1* (mouse) 5'-TAACTTCCTCACTCGAAGCCA-3' (forward), and 5'-AGTTCCATGACCCATCTCTGTC-3' (reverse); *RXRα* (human) 5'-ATGGACACCAAACATTTCCTGC-3' (forward), and 5'-GGGAGCTGATGACCGAGAAAG-3' (reverse); *Acox1* (human) 5'-AATCGGGACCCATAAGCCTTT-3' (forward),

and 5'-GGGAATACGATGGTTGTCCATTT-3' (reverse); *18S* 5'-GTCTGTGATGCCCTTAGATG-3' (forward) and 5'-AGCTTATGACCCGCACTTAC-3' (reverse). For miR-124 detection, RNA was extracted using a miRNeasy Mini Kit (Qiagen China Co., Ltd., Shanghai, China) according to the manufacturer's instructions. cDNA was synthesized by reverse transcription (RT) with a miScript RT II kit (Qiagen China Co.). Quantitative RT-PCR was performed using a miScript SYBR-Green PCR kit (Qiagen China Co.), and primers for miR-124 (MS00029211 and MS00006622) and RNU6-2 (MS00033740; all from Qiagen China Co.) were used according to the manufacturer's instructions. Relative mRNA expression levels were determined by the ΔΔCq method using 18S/RNU6-2 expression levels for normalization (12).

Immunoblotting assays. Tissues were lysed in tissue lysis buffer [20 mM Tris/HCl (pH 7.5), 4 mM EDTA (pH 8.0), 2% SDS] and cells were lysed in RIPA [20 mM Tris/HCl (pH 7.5), 150 mM NaCl, 1 mM EDTA, 1% NP-40, 0.5% sodium deoxycholate, 0.1% SDS] supplemented with protease inhibitors and phosphatase inhibitor cocktails (Roche Diagnostics, Indianapolis, IN, USA). Western blot analysis was performed according to routine procedure. Proteins were quantified using the BCA method. Samples containing 50 μg protein were separated by 10% SDS-PAGE and transferred to polyvinylidene difluoride (PVDF) membranes (EMD Millipore, Billerica, MA, USA). The membranes were blocked with 5% Difco™ Skim Milk (cat. no. 232100; BD Difco, Franklin Lakes, NJ, USA) for 1 h at room temperature. Then, the membranes were incubated overnight at 4˚C with the specific antibodies. Antibodies used were as follows: Anti-Stat3 (dilution 1:1,000; cat. no. 4904), anti-AKT (dilution 1:1,000; cat. no. 9272), anti-4E-BP1 (dilution 1:1,000; cat. no. 9644), anti-p70 S6K (dilution 1:1,000; cat. no. 2708) (all from Cell Signaling Technology, Inc., Beverly, MA, USA), anti-α-Tubulin (dilution 1:1,000; cat. no. Ab102; Vazyme, Nanjing, China) and anti-RXRα (dilution 1:1,000; cat. no. 21218; ProteinTech Group, Inc., Chicago, USA). Membranes were incubated with anti-mouse IgG, HRP-linked antibody (dilution 1:5,000; cat. no.7076P2; Cell Signaling Technology, Inc.) or anti-rabbit IgG, HRP-linked antibody (dilution 1:5,000; cat. no. 7074P2; Cell Signaling Technology, Inc.) for 1 h at room temperature. Immunocomplexes were visualized with ECL and visualized by Tanon Chemiluminescent Imaging System (Tanon Science and Technology Co., Shanghai, China).

Dual-Luciferase reporter assay. 293T cells were cultured in 96-well plates and co-transfected with 10 ng pMIR-RXRα 3'-UTR wild-type (WT), pMIR-RXRα 3'-UTR mutant type 1594-1600 (MT1) or pMIR-RXRα 3'-UTR mutant type 2700-2706 (MT2) and 5 pmol miR-124 mimics or negative control. After a 48-h incubation, *Renilla* luciferase activities were measured using the Dual-Luciferase Reporter Assay system (Promega Corp., Madison, WI, USA).

Immunohistochemical staining analysis. Sections were deparafnized, incubated with primary antibodies (RXRα, dilution 1:1,000; cat. no. 21218; Proteintech, IL, Chicago, USA). A subsequent reaction was performed with biotin-free HRP enzyme-labeled polymer from an EnVision Plus detection system (Dako; Agilent Technologies, Inc., Santa Clara, CA, USA). Positive reactions were visualized with diaminobenzidine (DAB) solution followed by counterstaining with hematoxylin. Sections were observed under light microscopy and the staining intensity scores were independently assessed by 2 pathologists.

Statistical analysis. All data are presented as the means ± SEM. Statistical calculations were performed using GraphPad Prism 5 (GraphPad Software, Inc., San Diego, CA, USA). Student's t-test and one-way analysis of variance (ANOVA) followed by Dunnett's multiple comparisons test were used, respectively. Pearson's χ^2 test was performed to analyze the correlation between p-S6 expression and RXRα. All statistical analysis was carried out using SAS (version 9.0; SAS Institute, Inc., Cary, NC, USA). Values of $P<0.05$ were considered to indicate a statistically significant result.

Results

miR-124 promotes the apoptosis of TSC2-deficient cells. To verify whether miR-124 regulated LAM progression, a TSC2 wild-type and a TSC2-null stable cell line were used to mimic healthy and LAM cell models, respectively. At 48 h after transfection with miR-124 mimics, the apoptosis of TSC2-null cells was significantly induced (Fig. 1A, B and E). In comparison, miR-124 mimics slightly influenced TSC2 wild-type cells. To further validate our hypothesis, 621-101 cells, another TSC2-deficient cell line, were treated with miR-124 mimics and cell apoptosis was assessed. The results revealed that cell apoptosis was significantly induced (Fig. 1C, D and F). Collectively, TSC2-deficient cells were more sensitive to miR-124-induced cell apoptosis.

Rapamycin does not reverse miR-124-induced TSC2-null cell apoptosis. To explain why miR-124 selectively induced the apoptosis of TSC2-deficient cells, we treated TSC2-null cells with rapamycin to reduce mTORC1 activity. The results revealed that the apoptosis of TSC2-null cells treated with or without rapamycin was not markedly changed, indicating that rapamycin could not prevent cell apoptosis of TSC2-null cells induced by miR-124 (Fig. 2A-C). Recent studies (6,13,14) have reported that STAT3 and AKT are targets of miR-124 in colorectal cancer and hepatocellular carcinoma. We therefore detected the expression of STAT3, AKT, 4E-BP1 and p70 S6K under miR-124 overexpression. As revealed in Fig. 2D and E, null cells exhibited no significant difference in their expression. The aforementioned results demonstrated that miR-124 induced TSC2-null cell apoptosis via an mTORC1-independent manner.

RXRα is a direct target of miR-124 in TSC2 null cells. Then, we compared the transcriptome between TSC2 wild-type and null cells. The cDNA microarray analyses revealed 3,272 genes with a fold change >3 in TSC2-null cells compared with that in TSC2 wild-type cells when miR-124 was overexpressed (Fig. 3A). Combination with TargetScan prediction (http://www.targetscan.org/) and the annotation of Gene Ontology Biological Function (http://geneontology.org/), 12 candidates involved in cell growth were further

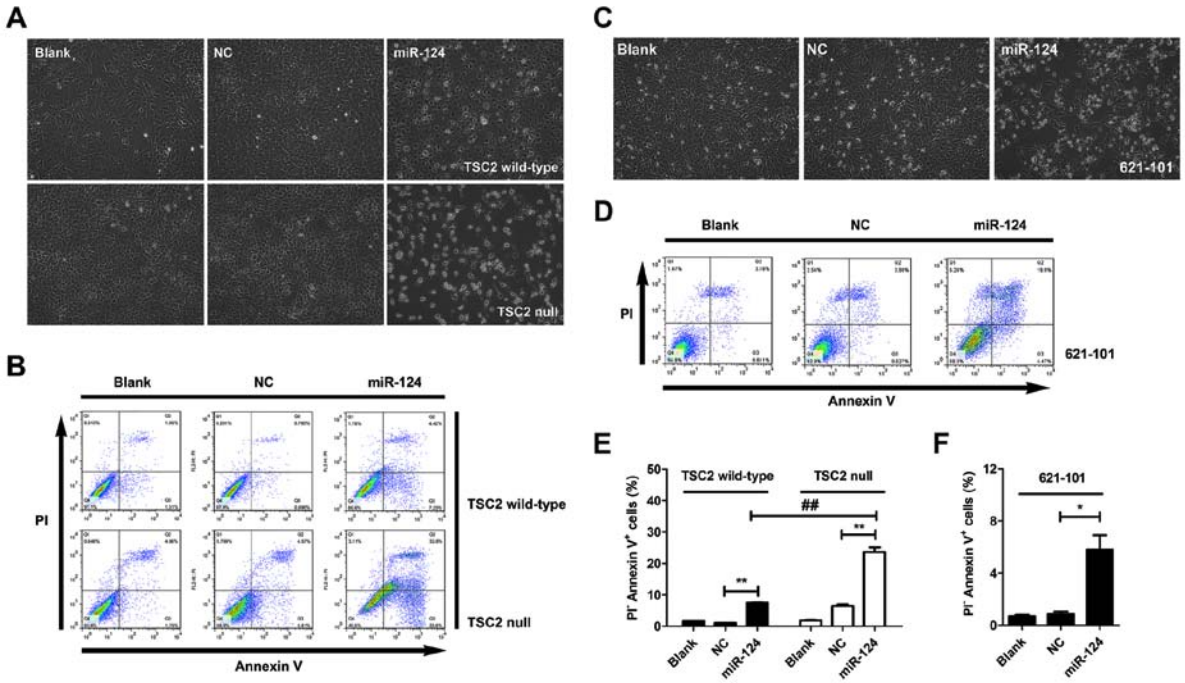

Figure 1. miR-124 promotes apoptosis of TSC2-deficient cells. At 48 h after transfection with miR-124 mimics or negative control (NC), cell apoptosis was observed and detected by flow cytometry. (A) Cellular morphology of apoptotic TSC2 wild-type and TSC2-null cells. (B) Representative flow cytometric results of TSC2 wild-type and TSC2-null cells. (C) Cellular morphology of apoptotic LAM patient-derived 621-101 cells. (D) Representative flow cytometric results of 621-101 cells (E) Quantification of apoptosis in B. (F) Quantification of apoptosis in D. LAM, lymphangioleiomyomatosis. *P<0.05, $^{**,\#\#}$P<0.01.

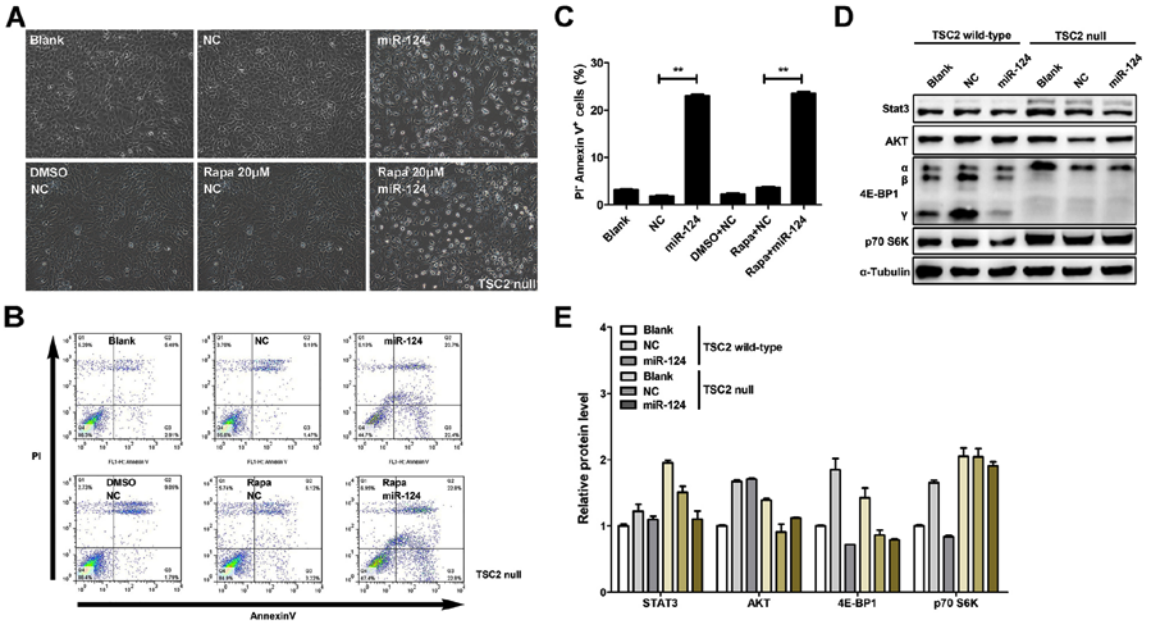

Figure 2. Rapamycin does not reverse miR-124-induced TSC2-null cell apoptosis. Cellular morphology of TSC2-null cells 48 h after incubation with miR-124 mimics/NC or rapamycin/DMSO. (B) Representative flow cytometric results of apoptosis in A. (C) Quantification of apoptosis in B. (D) Protein levels of Stat3, AKT, 4E-BP1 and p70 S6K in TSC2 wild-type and TSC2-null cells 48 h after transfection with miR-124 mimics and/or NC. (E) Quantification of the protein level in D. NC, negative control. **P<0.01.

investigated (Fig. 3B). Among these genes, RXRα mRNA was significantly downregulated by miR-124 in TSC2 wild-type and null cells (Fig. 3C). Additionally, restoration of RXRα reversed miR-124-induced apoptosis of TSC2-null cells (Fig. 3D and E), implying that miR-124 causes the apoptosis of TSC2-null cells via RXRα.

To further validate whether RXRα was directly regulated by miR-124, we introduced WT) or MT 3'-UTR (1594-1600 and 2700-2706) of RXRα into luciferase reporter plasmids. The WT and MT binding sequences are presented in Fig. 3F. Reporter assays revealed that miR-124 significantly decreased the luciferase activity of WT RXRα 3'-UTR, but not that of

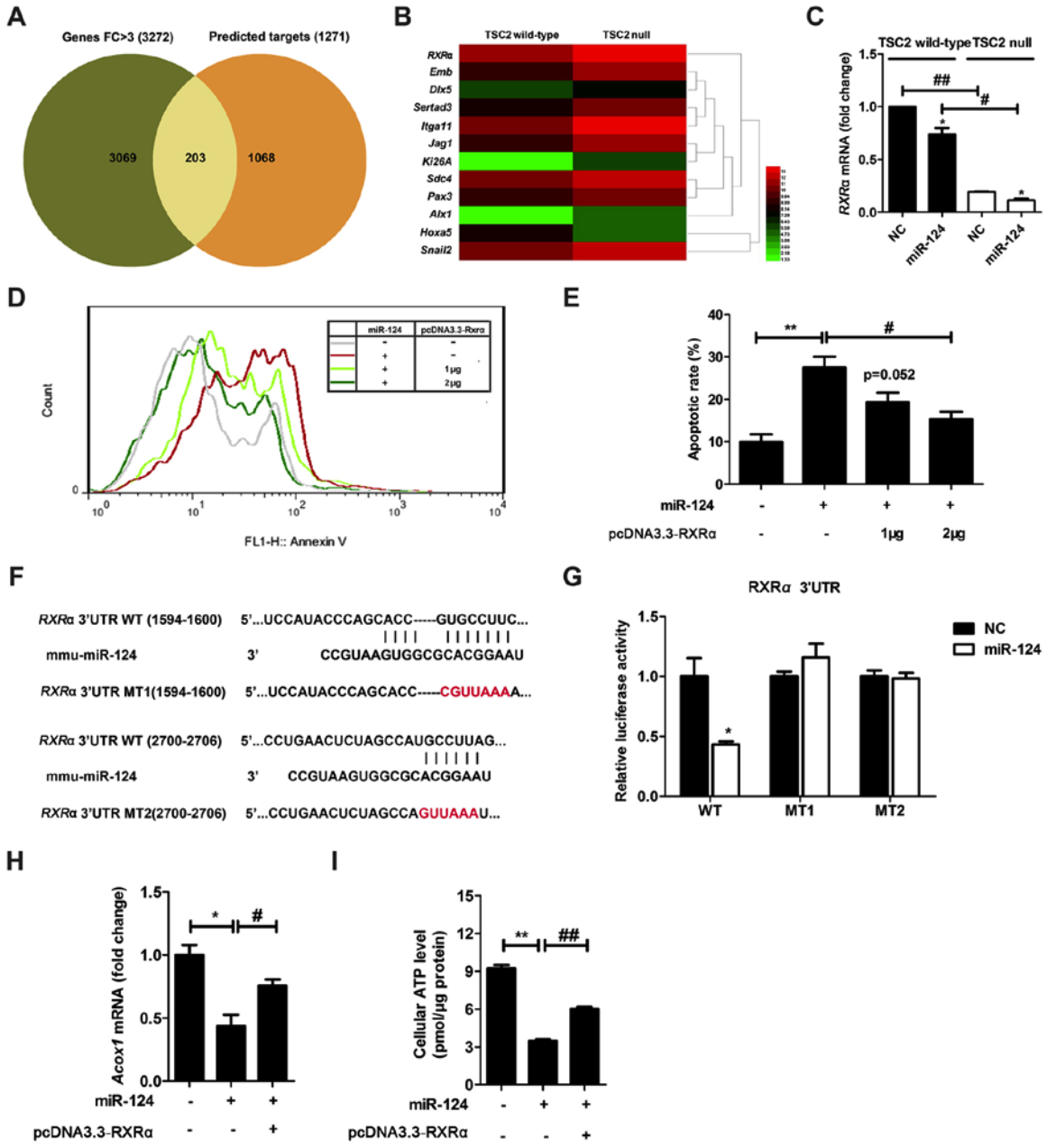

Figure 3. miR-124 promotes apoptosis of TSC2-null cells via *RXRα*. (A) cDNA microarray analyses revealed 3,272 genes with a fold change >3 in TSC2-null cells compared with that in TSC2 wild-type cells. (B) Heatmap of candidates regulating apoptosis of TSC2-null cells after miR-124 overexpression. (C) Expression of *RXRα* mRNA in TSC2 wild-type and TSC2-null cells 48 h after transfection with miR-124 mimics or NC. (D and E) The apoptosis of TSC2-null cells 48 h after transfection with miR-124 or pcDNA3.3-*RXRα*. (F) Diagram of miR-124 putative binding sites on the 3'-UTRs of *RXRα*. The mutant sequences used in the luciferase reporters are indicated in red. (G) Relative activity of luciferase reporters with *RXRα* 3'-UTR after co-transfection with miR-124 mimics or NC (50 nM) in 293T cells. Data were normalized to the levels in the corresponding negative control. (H and I) Expression of (H) Acox1, and (I) cellular ATP levels in TSC2-null cells 48 h after transfection with miR-124 mimics or *RXRα*. Representative results from 3 independent experiments are presented as the mean ± SEM. $^{*,\#}$P<0.05, $^{**,\#\#}$P<0.01. *RXRα*, retinoid X receptor α; NC, negative control; 3'-UTRs, 3'-untranslated regions.

2 MT RXRα 3'-UTR (Fig. 3G), indicating specific binding between miR-124 and RXRα 3'-UTR at both sites. Collectively, these data supported our hypothesis that RXRα is a direct target of miR-124.

The miR-124/RXRα axis regulates cell growth and fatty acid oxidation in TSC2-null cells in vivo. The RXRα/PPARα heterodimer is required for PPARα transcriptional activity on fatty acid oxidation genes such as *Acox1* (Acyl-CoA oxidase 1) (15). Thus, we detected the expression of Acox1 in TSC2-null cells. The results revealed that *Acox1* was suppressed when miR-124 was overexpressed, which was reversed by RXRα reconstitution (Fig. 3H). Additionally, ATP levels exhibited a similar tendency (Fig. 3I), further implying that miR-124/RXRα may mediate fatty acid oxidation of TSC2-null cells.

Next, we studied the effects of miR-124 on the growth of TSC2-null cells *in vivo*. The TSC2-null cells (referred to TSC2-null-tet-124) with a Tet-On system to overexpress miR-124 were injected into nude mice (Fig. 4A). At 7 days

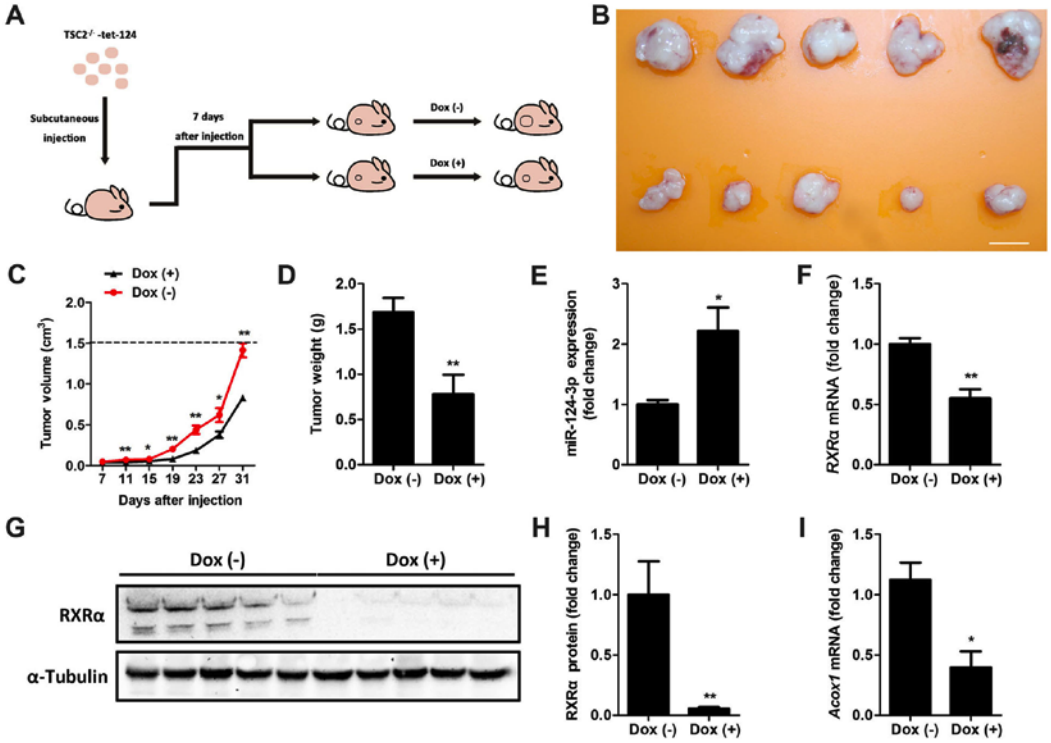

Figure 4. The miR-124/RXRα axis regulates growth of TSC2-null cells *in vivo*. (A) A schematic flowchart for xenograft assays in nude mice. (B) Representative images of xenograft tumors with or without Dox treatment. Scale bar, 1 cm. (C and D) Tumor (C) volume and (D) weight of xenograft tumors with or without Dox treatment (n=7 of each group). (E and F) Expression of *miR-124*, and *RXRα* mRNA in xenograft tumors with or without Dox treatment (n=7 of each group). (G and H) Protein levels of RXRα in xenograft tumors with or without Dox treatment. (I) Expression of *Acox1* mRNA in xenograft tumors with or without Dox treatment (n=7 of each group). Representative results out of 3 independent experiments are presented as mean ± SEM. *P<0.05, **P<0.01. Dox, doxycycline; RXRα, retinoid X receptor α.

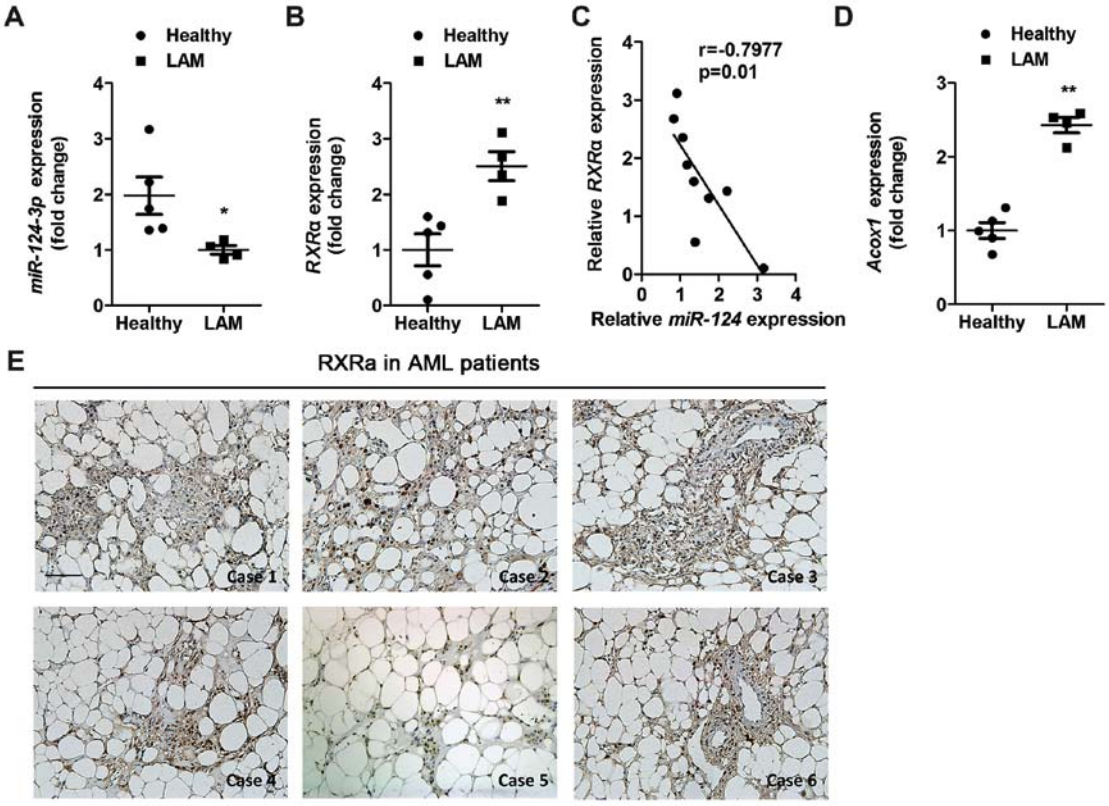

Figure 5. Dysregulation of miR-124/RXRα in LAM patients. (A and B) Expression of (A) *miR-124* and (B) *RXRα* in LAM tissues (n=4) and healthy controls (n=5). (C) Linear regression of *miR-124* and *RXRα* in LAM tissues (n=4) and healthy controls (n=5). (D) Expression of *Acox1* in LAM tissues (n=4) and healthy controls (n=5). (E) Representative images of areas with immunohistochemical staining of RXRα in AML tissues. Scale bars, 200 μm. Representative results from 3 independent experiments are presented as the mean ± SEM. *P<0.05, **P<0.01. RXRα, retinoid X receptor α; LAM, lymphangioleiomyomatosis; AML, angiomyolipoma.

Table I. RXRα is upregulated in mTORC1-hyperactive AML patients.

		RXRα		
Variable	Intensity	Positive	Negative	P-value
p-S6	0	0	3	0.035
	1	5	11	
	2	7	11	
	3	4	0	
Total		16	25	41

The scores (0, 1, 2 and 3) are based on the staining intensity of p-S6. RXRα, retinoid X receptor α; mammalian target of rapamycin complex 1; AML, angiomyolipoma.

after injection, the expression of miR-124 was induced with Dox (Dox^+) or not induced (Dox^-). We found that compared with Dox^- group, mice in the Dox^+ group revealed significantly reduced tumor volume and weight at 31 days after injection (Fig. 4B-D). However, body weights of $Dox^{+/-}$ mice revealed no significant difference (data not shown). We further examined the expression of miR-124 and RXRα in a xenograft tumor. As expected, Dox-treated xenograft tumors expressed significantly higher miR-124 levels and lower *RXRα*/*Acox1* levels compared to those in the control group (Fig. 4E, F and I). Western blot assays also revealed that RXRα exhibited a markedly reduced level in miR-124-overexpressing xenograft tumors (Fig. 4G and H). Therefore, these findings indicated that the miR-124/RXRα axis regulated the growth of TSC2-null cells *in vivo*.

Dysregulation of miR-124/RXRα in LAM patients. To further address the significance of the miR-124/RXRα pathway, we performed quantitative real-time PCR to examine the expression of miR-124 and RXRα in LAM-patient-derived tissues (n=4). The results revealed a significant decrease of miR-124 expression in LAM samples compared to that in healthy controls (Fig. 5A), whereas the mRNA levels of *RXRα* and *Acox1* were significantly upregulated (Fig. 5B and D). However, linear regression analysis of *miR-124* and *RXRα* (Fig. 5C) was also performed. The results revealed a negative correlation between *miR-124* and *RXRα*, further indicating that *RXRα* is an important target of miR-124 in LAM. The expression of RXRα in AML tissues was further analyzed and it was revealed that, the marker of mTORC1 activation, phosphorylation of S6 was negatively correlated with the expression of RXRα (Fig. 5E and Table I). Patients with higher mTORC1 activity expressed more RXRα. These results indicated that miR-124/RXRα may serve as a promising biomarker for LAM patients.

Discussion

The Multicenter International LAM Efficacy and Safety of Sirolimustrial (MILES) trial demonstrated that sirolimus is associated with the reduction of symptoms and improvement of life quality by stabilizing lung function (16). However, after discontinuation of sirolimus, the decline in lung function resumed, similar to untreated patients (17). These findings indicated that temporarily retarding progression rather than eradicating LAM cells leads to LAM relapse, causing LAM at an alarming rate. In the present study, we found that miR-124 induced the apoptosis of TSC2-deficient cells via targeting of RXRα-mediated peroxisomal fatty acid oxidation. However, it was observed that miR-124 slightly affected TSC2 wild-type cells. Additionally, overexpression of miR-124 reduced the growth of TSC2-deficient cell-induced xenograft tumors. Moreover, we observed significantly decreased miR-124 and elevated *RXRα* and *Acox1* expression levels in LAM samples compared to those in the healthy control group. Our results provided valuable clues for understanding the suppressive functions and mechanisms of miR-124 in LAM. Moreover, expression of miR-124 and RXRα may serve as a promising biomarker for LAM patients.

Changes in miRNA profiling are implicated in various human diseases such as LAM (18,19). However, whether miRNAs contribute to LAM therapy remains to be elucidated. Previous studies have reported that miR-124 was frequently decreased in tumors and functioned as a tumor suppressor, participating in cell proliferation, invasion and inflammation (11,20). Silencing of miR-124 induced the apoptosis of neuroblastoma SK-N-SH cells by promoting aryl hydrocarbon receptor. It has also been revealed that miR-124 mimics induced cell apoptosis in prostate and gastric cancer, and Parkinson's disease (17,21,22). In the present study, we found that overexpression of miR-124 resulted in apoptosis of TSC2-deficient cells, which was reversed by restoration of RXRα. In a TSC2-null cell-induced xenograft, miR-124 markedly suppressed tumor growth by suppressing *RXRα*/*Acox1*. Further study could focus on testing toxicity of miR-124 and a TSC2-null cell-induced spontaneous LAM mouse model could be used (23).

RXRs (α, β and γ) are the master coordinators of cell growth, metabolism, and development (24,25). The RXRα/PPARα heterodimer is required for transcriptional activity on fatty acid oxidation genes such as *Acox1* (26). Inhibition of fatty acid oxidation by etomoxir was revealed to impair NADPH production and increase reactive oxygen species resulting in ATP depletion and cell death in human glioblastoma cells (27). However, attenuated fatty acid oxidation sensitized human leukemia cells to apoptosis induction (28). In the present study, we revealed that RXRα was a direct target of miR-124 and mediated miR-124-induced apoptosis in TSC2-deficient cells, indicating that RXRα-regulated peroxisomal fatty acid oxidation may play a vital role in LAM growth. In addition, miR-124 slightly affected TSC2 wild-type cells, which ensured low toxicity to healthy cells during LAM therapy. Limiting energy supply through miR-124/RXRα may be a promising therapy for LAM. In addition, the RXR-RAR heterodimers are associated with histone acetylation, chromatin condensation and transcriptional regulation (29), regulating cell survival. Thus, follow-up studies should focus on discovering the specific mechanisms by which RXR regulates LAM apoptosis.

In conclusion, our study provided novel evidence that miR-124 induced apoptosis of TSC2-deficient cells by suppressing RXRα and fatty acid oxidation. Our results indicated that miR-124 could be a potential target for the future treatment of LAM.

Acknowledgements

The authors thank Dr John Blenis for providing TSC2 wild-type and TSC2-null cells. In addition, the authors would like to thank the Translational Medicine Core Facilities, Medical School of Nanjing University for instrumental support, and the Liver Disease Collaborative Research Platform of Medical School, Nanjing University for discussion.

Funding

The present study was supported by the Chinese National Science Foundation (nos. 31371373 and 31771572), the Nature Science Foundation of Jiangsu Province (no. BK20151395), the Open Fund of State Key Laboratory of Natural Medicines (no. SKLNMKF201606), the Fundamental Research Funds for the Central Universities (021414380330), the Priority Academic Program Development of Jiangsu Higher Education Institutions (PAPD) and the National Natural Science Foundation of China (31100448).

Availability of data and materials

The datasets used during the present study are available from the corresponding author upon reasonable request.

Authors' contributions

JL and BX conceived the study and were responsible for the experimental design. JL, JY, TF, YZ, QS performed the experiments. JuC, JiC and MJ collected the human samples and assisted with their analysis. JL and BX interpreted the data and wrote the manuscript. All authors read and approved the manuscript and agree to be accountable for all aspects of the research in ensuring that the accuracy or integrity of any part of the work are appropriately investigated and resolved.

Ethics approval and consent to participate

All protocols for humans were reviewed and approved by the Ethical Committee of Nanjing University (Nanjing, China). Written informed consent was obtained from all patients for the use of their clinical tissues. All animal procedures were carried out in accordance with the approval of the Animal Care and Use Committee at the Model Animal Research Center of Nanjing University.

Patient consent for publication

Not applicable.

Competing interests

The authors state that they have no competing interests.

References

1. Taveira-DaSilva AM, Steagall WK and Moss J: Lymphangioleiomyomatosis. Cancer Control 13: 276-285, 2006.
2. Yamazaki A, Miyamoto H, Futagawa T, Oh W, Sonobe S, Takahashi N, Izumi H, Hirama M, Seyama K and Fukuchi Y: An early case of pulmonary lymphangioleiomyomatosis diagnosed by video-assisted thoracoscopic surgery. Ann Thorac Cardiovasc Surg 11: 405-407, 2005.
3. Chang WY, Cane JL, Blakey JD, Kumaran M, Pointon KS and Johnson SR: Clinical utility of diagnostic guidelines and putative biomarkers in lymphangioleiomyomatosis. Respir Res 13: 34, 2012.
4. Singer CA, Barnett SD, Grubbs J and Camoretti-Mercado B: MiR-25 targeting tuberous sclerosis complex 1 (TSC1) expression in lymphangioleiomyomatosis cells. In: A63. Advances in lymphangioleiomyomatosis and tuberous sclerosis: Bench to Bedside American Thoracic Society, 187: ppA2027, 2013.
5. Di Leva G, Garofalo M and Croce CM: MicroRNAs in cancer. Annu Rev Pathol 9: 287-314, 2014.
6. Lang Q and Ling C: MiR-124 suppresses cell proliferation in hepatocellular carcinoma by targeting PIK3CA. Biochem Biophys Res Commun 426: 247-252, 2012.
7. Furuta M, Kozaki KI, Tanaka S, Arii S, Imoto I and Inazawa J: miR-124 and miR-203 are epigenetically silenced tumor-suppressive microRNAs in hepatocellular carcinoma. Carcinogenesis 31: 766-776, 2010.
8. Kim VN, Han J and Siomi MC: Biogenesis of small RNAs in animals. Nat Rev Mol Cell Biol 10: 126-139, 2009.
9. Xu X, Li S, Lin Y, Chen H, Hu Z, Mao Y, Xu X, Wu J, Zhu Y, Zheng X, *et al*: MicroRNA-124-3p inhibits cell migration and invasion in bladder cancer cells by targeting ROCK1. J Transl Med 11: 276, 2013.
10. Qiu Z, Guo W, Wang Q, Chen Z, Huang S, Zhao F, Yao M, Zhao Y and He X: MicroRNA-124 reduces the pentose phosphate pathway and proliferation by targeting *PRPS1* and *RPIA* mRNAs in human colorectal cancer cells. Gastroenterology 149: 1587-1598.e11, 2015.
11. Liang YJ, Wang QY, Zhou CX, Yin QQ, He M, Yu XT, Cao DX, Chen GQ, He JR and Zhao Q: MiR-124 targets Slug to regulate epithelial-mesenchymal transition and metastasis of breast cancer. Carcinogenesis 34: 713-722, 2013.
12. Livak KJ and Schmittgen TD: Analysis of relative gene expression data using real-time quantitative PCR and the $2^{-\Delta\Delta CT}$ method. Methods 25: 402-408, 2001.
13. Koukos G, Polytarchou C, Kaplan JL, Morley-Fletcher A, Gras-Miralles B, Kokkotou E, Baril-Dore M, Pothoulakis C, Winter HS and Iliopoulos D: MicroRNA-124 regulates STAT3 expression and is down-regulated in colon tissues of pediatric patients with ulcerative colitis. Gastroenterology 145: 842-852. e2, 2013.
14. Zhang J, Lu Y, Yue X, Li H, Luo X, Wang Y, Wang K and Wan J: MiR-124 suppresses growth of human colorectal cancer by inhibiting STAT3. PLoS One 8: e70300, 2013.
15. Gorla-Bajszczak A, Juge-Aubry C, Pernin A, Burger AG and Meier CA: Conserved amino acids in the ligand-binding and tau(i) domains of the peroxisome proliferator-activated receptor alpha are necessary for heterodimerization with RXR. Mol Cell Endocrinol 147: 37-47, 1999.
16. Young L, Lee HS, Inoue Y, Moss J, Singer LG, Strange C, Nakata K, Barker AF, Chapman JT, Brantly ML, *et al*: Serum VEGF-D a concentration as a biomarker of lymphangioleiomyomatosis severity and treatment response: A prospective analysis of the multicenter international lymphangioleiomyomatosis efficacy of sirolimus (MILES) trial. Lancet Respir Med 1: 445-452, 2013.
17. Shi XB, Xue L, Ma AH, Tepper CG, Gandour-Edwards R, Kung HJ and deVere White RW: Tumor suppressive miR-124 targets androgen receptor and inhibits proliferation of prostate cancer cells. Oncogene 32: 4130-4138, 2013.
18. Ito Y, Inoue A, Seers T, Hato Y, Igarashi A, Toyama T, Taganov KD, Boldin MP and Asahara H: Identification of targets of tumor suppressor microRNA-34a using a reporter library system. Proc Natl Acad Sci USA 114: 3927-3932, 2017.
19. Lam HC, Liu HJ, Baglini CV, Filippakis H, Alesi N, Nijmeh J, Du H, Lope AL, Cottrill KA, Handen A, *et al*: Rapamycin-induced miR-21 promotes mitochondrial homeostasis and adaptation in mTORC1 activated cells. Oncotarget 8: 64714-64727, 2017.

20. Zheng F, Liao YJ, Cai MY, Liu YH, Liu TH, Chen SP, Bian XW, Guan XY, Lin MC, Zeng YX, *et al*: The putative tumour suppressor microRNA-124 modulates hepatocellular carcinoma cell aggressiveness by repressing ROCK2 and EZH2. Gut 61: 278-289, 2012.
21. Xie L, Zhang Z, Tan Z, He R, Zeng X, Xie Y, Li S, Tang G, Tang H and He X: MicroRNA-124 inhibits proliferation and induces apoptosis by directly repressing EZH2 in gastric cancer. Mol Cell Biochem 392: 153-159, 2014.
22. Gong X, Wang H, Ye Y, Shu Y, Deng Y, He X, Lu G and Zhang S: miR-124 regulates cell apoptosis and autophagy in dopaminergic neurons and protects them by regulating AMPK/mTOR pathway in Parkinson's disease. Am J Transl Res 8: 2127-2137, 2016.
23. Goncharova EA, Goncharov DA, Fehrenbach M, Khavin I, Ducka B, Hino O, Colby TV, Merrilees MJ, Haczku A, Albelda SM and Krymskaya VP: Prevention of alveolar destruction and airspace enlargement in a mouse model of pulmonary lymphangioleiomyomatosis (LAM). Sci Transl Med 4: 154ra134, 2012.
24. Mangelsdorf DJ, Ong ES, Dyck JA and Evans RM: Nuclear receptor that identifies a novel retinoic acid response pathway: Nature 345: 224-229, 1990.
25. De Luca LM: Retinoids and their receptors in differentiation, embryogenesis, and neoplasia. FASEB J 5: 2924-2933, 1991.
26. Varanasi U, Chu R, Huang Q, Castellon R, Yeldandi AV and Reddy JK: Identification of a peroxisome proliferator-responsive element upstream of the human peroxisomal fatty acyl coenzyme A oxidase gene. J Biol Chem 271: 2147-2155, 1996.
27. Pike LS, Smift AL, Croteau NJ, Ferrick DA and Wu M: Inhibition of fatty acid oxidation by etomoxir impairs NADPH production and increases reactive oxygen species resulting in ATP depletion and cell death in human glioblastoma cells. Biochim Biophys Acta 1807: 726-734, 2011.
28. Samudio I, Harmancey R, Fiegl M, Kantarjian H, Konopleva M, Korchin B, Kaluarachchi K, Bornmann W, Duvvuri S, Taegtmeyer H, *et al*: Pharmacologic inhibition of fatty acid oxidation sensitizes human leukemia cells to apoptosis induction. J Clin Invest 120: 142-156, 2010.
29. Minucci S, Horn V, Bhattacharyya N, Russanova V, Ogryzko VV, Gabriele L, Howard BH and Ozato K: A histone deacetylase inhibitor potentiates retinoid receptor action in embryonal carcinoma cells. Proc Natl Acad Sci USA 94: 11295-11300, 1997.